Selective Mott Physics as a Key to Iron Superconductors

Luca de' Medici,[1,2,3] Gianluca Giovannetti,[4] and Massimo Capone[4]
[1]Laboratoire de Physique et Etude des Matériaux, UMR8213 CNRS/ESPCI/UPMC, Paris, France
[2]Laboratoire de Physique des Solides, UMR8502 CNRS-Université Paris-Sud, Orsay, France
[3]European Synchrotron Radiation Facility, BP 220, F-38043 Grenoble Cedex 9, France
[4]CNR-IOM-Democritos National Simulation Centre and International School for Advanced Studies (SISSA), Via Bonomea 265, I-34136, Trieste, Italy
(Received 17 October 2013; published 28 April 2014)

We show that electron- and hole-doped $BaFe_2As_2$ are strongly influenced by a Mott insulator that would be realized for half-filled conduction bands. Experiments show that weakly and strongly correlated conduction electrons coexist in much of the phase diagram, a differentiation which increases with hole doping. This selective Mottness is caused by the Hund's coupling effect of decoupling the charge excitations in different orbitals. Each orbital then behaves as a single-band doped Mott insulator, where the correlation degree mainly depends on how doped is each orbital from half filling. Our scenario reconciles contrasting evidences on the electronic correlation strength, implies a strong asymmetry between hole and electron doping, and establishes a deep connection with the cuprates.

DOI: 10.1103/PhysRevLett.112.177001 PACS numbers: 74.70.Xa, 71.27.+a, 71.30.+h, 74.20.Pq

High-T_c superconductivity is the most spectacular example of a wide palette of unconventional behaviors induced by electronic correlations. The latter are indeed identified as the origin of both the Mott insulating parent compound and of the superconducting pairing in the cuprates. In this light, the question of the correlation strength in iron superconductors [1], the runner-up materials in terms of T_c (up to 57 K), is crucial and remains to be clarified. Despite a bad metallic conductivity and many other unconventional properties [2,3], experiments have hardly detected any general direct signature of strong local interactions such as a Hubbard band [4] and have instead reported an overall fair agreement with density functional theory (DFT) predictions and assessed the local screened Coulomb repulsion U in the d orbitals to be smaller than the total width of the conduction bands $W \sim 4$ eV. This led to theories starting either from the weak-coupling [5] or from the strong-coupling [6] pictures.

On the other hand, it has been emphasized early on that [7] that Hund's coupling J plays a major role in determining the degree of correlations in these materials. This term, which favors high-spin configurations on each atom, is consistently estimated to be ~0.3 to 0.6 eV (in standard Kanamori notation) both theoretically and experimentally. On general grounds, it has been found [8] that for the filling of six electrons in five orbitals J favors a bad-metallic behavior yet pushing away the Mott insulator. It has also been shown [7] that this kind of correlated metal does not display as prominent Hubbard bands as in standard correlated materials. Overall, an image of moderately strong correlations [9] driven by Hund's coupling, seems to emerge.

The evolution as a function of doping is the smoking gun of the relevance of Mott physics (Mottness) in the cuprates. Approaching half filling, the electronic motion is hindered leading to increasingly bad metals culminating in the pseudogap phase and eventually, in an actual Mott insulator.

In the present Letter, we use the doping dependence as a litmus paper to assess the role of correlations in iron superconductors. By collecting experimental data from different probes, we show that in the 122 family (i.e., both hole- and electron-doped $BaFe_2As_2$) the effective mass of the carriers increases as the filling decreases and the stoichiometric compound is not special in terms of correlation strength. This doping dependence is heavily differentiated among the electrons forming the conductions bands.

Our theoretical calculations will indeed show that the degree of correlation is determined by the distance to a Mott insulating state that would be realized with five electrons per iron atom. This effect is due to the dominance of the Hund's J, which in turn decouples the charge excitations in the different orbitals, so that the multiorbital system becomes effectively a collection of doped Mott insulators. Each of them happens to have a different population, which reflects in a different distance from the Mott state and in a different effective mass. This brings about a scenario of coexisting strongly and weakly correlated electrons. Indeed, it was shown by two of us that iron superconductors are the ideal ground for heavily orbital-dependent correlation effects (selective Mottness), or even for orbital-selective Mott localization [25,26]. Phenomenological descriptions assuming the presence of itinerant and localized electrons [27–29] have indeed reproduced many features of these materials.

Figure 1 displays experimental estimates of the mass enhancement from specific heat, infrared reflectivity, angle-resolved photoemission spectroscopy (ARPES), and

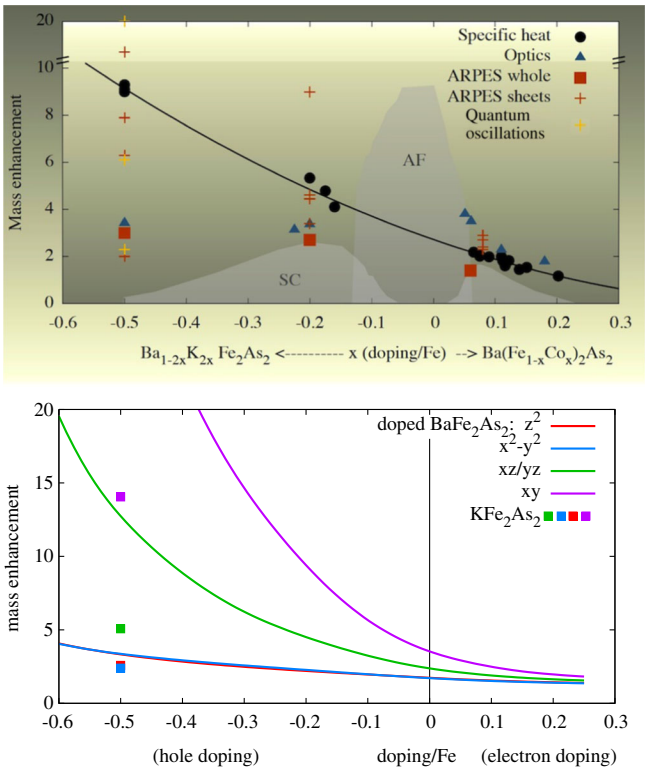

FIG. 1 (color online). Top: experimental mass enhancements in doped $BaFe_2As_2$ assessed by different techniques (see the Supplemental Material [30]) [10–24]. The experimental phase diagram, including the antiferromagnetic metallic (AF) and the superconducting (SC) phases is reproduced as a background. The solid line is a fit of the specific heat data. ARPES and quantum oscillation data corresponding to a given doping represent the values estimated for the different sheets of the Fermi surface. Correlations increase monotonically as the filling is reduced, and the estimates from different techniques spread more and more (see text). Bottom: orbitally resolved mass enhancement calculated within local-density approximation (LDA)+slave-spin mean-field theory for doped $BaFe_2As_2$ (lines) and for KFe_2As_2 (squares).

quantum oscillations (the references are detailed in the Supplemental Material [30]). All the data are taken in the high-temperature tetragonal metallic phase above the magnetically ordered (and orthorombically distorted) phase at low dopings and the superconducting one at intermediate dopings.

Single-crystal specific heat measurements delineate a very clear trend: the mass enhancement $m^*/m_b = \gamma/\gamma_b$ (where γ and γ_b are, respectively, the measured normal-state Sommerfeld coefficient and the band theory estimate $\gamma_b = \pi^2 k_B^2/3N_0$, N_0 being the total density of states at the Fermi energy) grows continuously from ~2 in the electron-overdoped $Ba(Fe_{1-x}Co_x)_2As_2$ to 3 in the electron underdoped and the stoichiometric compounds toward 5–6 in the optimally hole-doped $Ba_{1-x}K_xFe_2As_2$ until reaching the very high value of ~9 for the fully substituted KFe_2As_2 (having a doping of 0.5 holes/Fe).

Optical conductivity provides a partially different picture. Comparing the band theory estimate of the Drude weight

$$D_{\text{band}} = \sum_{\alpha,k} \left(\frac{\partial \epsilon_k^\alpha}{\partial k_x} \right)^2 \delta(\epsilon_k^\alpha - \epsilon_F), \tag{1}$$

(where ϵ_k^α is the dispersion of band α) with the experimental value, one obtains an optical effective mass $D_{\text{band}}/D_{\text{exp}} = m^*/m_b$. With this approach, Qazilbash *et al.* [31] found intermediate correlation strength (~3.3 for $BaFe_2As_2$) while the data we collect show correlations diminishing with electron doping but a possible saturation (with m^*/m_b hardly exceeding ~4) of the mass enhancement for the hole-doped compounds.

A general argument links this apparent discrepancy to the coexistence of electrons with different effective mass renormalization: in this multiband environment, both the conductivity and the density of states at the Fermi energy stem from a sum over the band (or orbital) index. As a consequence, $\gamma/\gamma_b = D_{\text{band}}/D_{\text{exp}}$ only if the mass enhancement is the same for all electrons. If instead the renormalization is different from band to band (from orbital to orbital), the density of states is a sum of contributions $\sim(m^*/m_b)_\alpha$, whereas the Drude weight is a sum of terms $\sim(m_b/m^*)_\alpha$, and thus as it happens for series or parallels of resistances, the first will be dominated by the largest mass enhancement, the second by the smallest. This means that in case of heavy differentiation of correlation strength, the enhancement of the Sommerfeld coefficient will reflect that of the strongly correlated electrons, whereas the Drude weight, the one of the weakly correlated ones. Moreover at finite temperatures, the heavier electrons tend to drop out from the low-frequency optical response because of their lower coherence.

A more direct confirmation of this picture is obtained by means of ARPES. In order to roughly match the experimental data, the DFT band structure has to be renormalized by a global factor (indicated as "ARPES whole" in Fig. 1) that increases with decreasing filling. Moreover, by measuring the Fermi velocity on the different Fermi sheets and comparing them to DFT calculations, one can estimate independently the mass enhancements of the corresponding low energy electrons. As we report in Fig. 1, in the electron-doped side of the phase diagram, the different Fermi sheets show a homogeneous renormalization of the Fermi velocities by a factor of order ~2, whereas moving to the hole-doped side the different Fermi sheets show different renormalization for different bands (between 3 and 9 for $Ba_{0.6}K_{0.4}Fe_2As_2$ and between 2 and 18 for KFe_2As_2). Quantum oscillations measurements performed on KFe_2As_2 also report a heavy differentiation between the mass enhancement.

Thus, in summary, the unified phase diagram of electron- and hole-doped $BaFe_2As_2$ shows a strong and monotonic increase of correlations going from the heavy electron

overdoping to the heavy hole overdoping, and a parallel progressive differentiation of the mass enhancements, or selective Mottness. It is also worth noting that the stoichiometric filling does not play a particular role in this phase diagram of the tetragonal phase, contrary to the fact that commensuration is naively expected to strengthen the effects of correlations.

Calculations including dynamical correlations in DFT *ab initio* calculations for both iron pnictides and chalcogenides show that the combined role of U and J gives rise to a novel scenario (as summarized in Ref. [33]). A sharp crossover [34–36] is found, as a function of increasing correlation strength and decreasing filling, toward a "Hund's metal" [37] state. The physics there is dominated by Hund's coupling and can be described using a few concepts isolated in model studies: (1) a strongly correlated metallic phase far from the Mott transition at $n = 6$ [8] is realized [35,36,38] with a very low coherence temperature and correlation strength more sensitive to J than to U [7]; (2) above such coherence temperature a "spin-frozen" state appears [39,40], in which the self-energy has a peculiar $\sqrt{\omega}$ dependence at low ω and long spin correlation time [41]; (3) "orbital decoupling" [42] happens, i.e., differentiation of the correlation strength among the different orbitals, due to the fact the Hund's coupling suppresses inter orbital correlations, rendering charge excitations in the various orbitals virtually independent from one another.

This last point is what we highlight here as the main reason for the experimental scenario we have detailed.

We have performed LDA+slave-spin mean-field (see "Methods" section in the Supplemental Material [30]) calculations at $T = 0$ starting from DFT band structures for doped $BaFe_2As_2$ in the tetragonal phase (see the Supplemental Material [30] for other iron superconductors). We have checked that for the interaction strength corresponding to the *ab initio* estimate, this compound displays the signature of the Hund's metal phase. Our results as a function of U (see the Supplemental Material [30]) show that $BaFe_2As_2$ lies around or just above a crossover to a correlated phase signaled by a fast drop in the quasiparticle weight Z, an increase of the interorbital spin correlation functions and decrease in the interorbital charge correlation functions, as reported in [35,36]. As expected in this regime, the correlation strengths are strongly differentiated among orbitals, with the t_{2g} orbitals more correlated the e_g ones; in particular, the xy orbital is the most correlated of all. This motivates the experimental observation from ARPES that at low energy (where bands are mainly of t_{2g} character), the band structure is more renormalized than at high energy (where both t_{2g} and e_g characters are present). This heavy-fermionic behavior might be turned into an incoherent phase at $T \neq 0$ and/or with a refined treatment of quantum fluctuations [39,40].

We have studied the evolution as a function of total density of the orbitally resolved mass enhancements (bottom panel in Fig. 1), quasiparticle weights $Z_\alpha = (m_b/m^*)_\alpha$, and populations, which are shown in Fig. 2. Correlations clearly increase continuously decreasing the total population, resulting in a more correlated hole-doped side compared to the electron-doped one [34,43,44]. The commensurate filling of $n = 6$ does not play any special role in this undistorted phase. Also, the differentiation of correlation strength increases with hole doping.

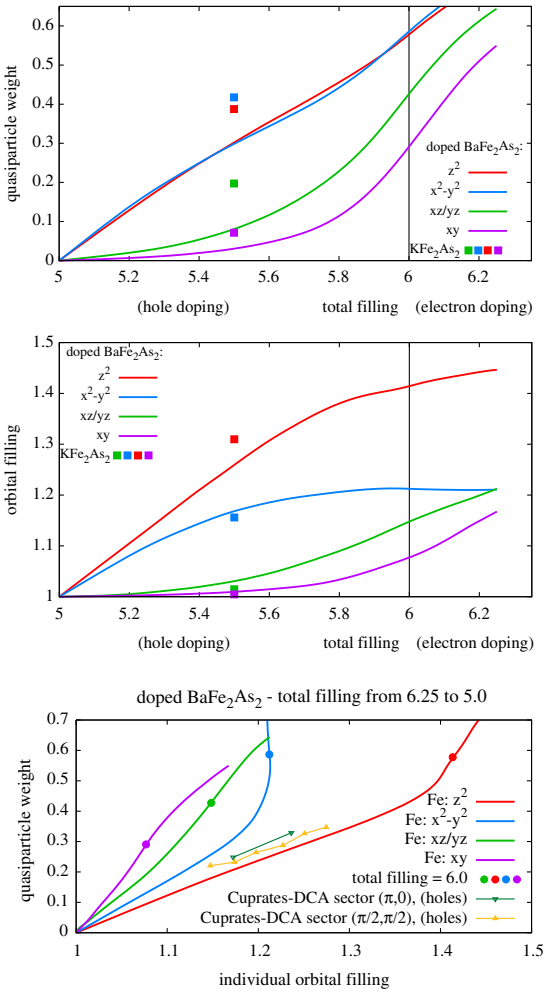

FIG. 2 (color online). Calculated orbitally resolved quasiparticle weight Z_α (upper panel) and electron population (middle panel) for doped $BaFe_2As_2$ and stoichiometric KFe_2As_2 (squares) within slave-spins mean field. Note that for each orbital α, Z_α tends to vanish when n_α approaches half filling. Indeed, when plotting Z_α as a function of n_α for each orbital (lower panel), a striking linear behavior (typical of a doped single-band Mott insulator) appears showing that each orbital is only sensitive to its doping away from the half-filled Mott insulator found at a total population $n = 5$, independently from the others. The dots signal the values for the stoichiometric compound, having a total population $n = 6$. The same analysis is performed for dynamical cluster approximation (DCA) calculations on the bidimensional Hubbard model of Gull *et al.* [32], representative of the pseudogap phase of underdoped cuprates, pointing to a common mechanism.

Thus, the calculations reproduce all the main trends of the experimental estimates (Fig. 1).

It can be noted that the theoretical mass enhancements reach values, for strong hole overdoping, much higher than experiments. This is explained by a progressive increase of covalency in the Fe-As planes introduced by the Ba → K substitution: when this is taken into account (using the DFT band structure for KFe_2As_2 at $n = 5.5$), correlation strengths close to the experimental values are obtained (colored squares in Figs. 1 and 2).

When the suggested orbital decoupling mechanism is realized, the system switches from a collective to an individual orbital behavior: the correlation strength in each orbital depends mainly on the doping of the orbital away from half filling. We have tested this hypothesis here and found that it is fully verified: in the lower panel of Fig. 2, we plot the quasiparticle weight of each orbital as a function of its population. Each orbital is mainly sensitive to its own filling and behaves like a doped single-band Mott insulator, with a Z characteristically proportional to the doping. With decreasing total population, all orbitals move toward half filling and the quasiparticle weights go to zero at $n = 5$, where the system is then a Mott insulator, with vanishing orbital polarization. The remarkable thing is that, albeit this happens at a very different rate for each orbital (the xy orbital is almost half filled already at $n = 6$, and thus, more strongly correlated, the z^2 is quite far from half filling until very close to $n = 5$, and thus, weakly correlated for most of the fillings), the behavior when plotted against the individual population is quite universal (the different slopes being determined by the details of the band structure).

This scenario confirms what has been observed in previous theoretical studies [34,44], that the parent compounds for pnictides at $n = 6$, are influenced by correlations due to the Mott insulator at $n = 5$. Here, we provide the reason why: the orbitals are decoupled from one another, thus rendering the individual population of each orbital crucial for its correlation strength. Accordingly, the seemingly far in population $n = 6$ compound, has orbitals instead very close to the Mott insulating state. The t_{2g} orbitals and the xy, in particular, are only a few percents of doping away from the selective Mott insulator. The coexistence of electrons whose different correlation degree descends from a different distance to the Mott insulator defines the selective Mottness and its role in the phase diagram.

One last more speculative hypothesis is now in order. By plotting the experimental phase diagram as a function of the average orbital population, the stoichiometric filling falls at 20% average doping [34]. This is now justified by the orbital-decoupled nature of the conduction electrons.

If, as quite generally believed, the magnetically ordered (and orthorhombically distorted) phase is detrimental to superconductivity [2] and it is favored accidentally by nesting and/or lack of disorder realized for the commensurate $n = 6$ filling, we can imagine that the unified phase diagram of the tetragonal phase of iron superconductors would see the two domes unified into a bigger one (see Fig. 3). This tentative phase diagram would now be strikingly similar to that of cuprate superconductors: a superconducting dome would be centered around a doping of 20% per band away from a Mott insulator and flanked at smaller doping by a bad metallic phase in which electrons with different correlation strength coexist, as it happens in hot or cold spots (culminating in the pseudogap phase) in the underdoped cuprates. At higher fillings, a weakly correlated good metal is recovered in both cases. Indeed, as detailed in the Supplemental Material [30], the momentum-space selectivity describing the hot or cold spot and the pseudogap phase of cuprates in the two-dimensional Hubbard model can be easily recast into a multiorbital effective picture within cluster extensions of dynamical mean-field methods [32]. The mass enhancement in each sector of the Brillouin zone scales linearly with the respective individual doping from half filling (Fig. 2, lower panel), signaling that the orbital-decoupling mechanism is at play and reminding the situation outlined for iron superconductors. This scenario unifies a series of seemingly contradictory evidences and it is expected to put serious constraints on pairing theories for superconductivity.

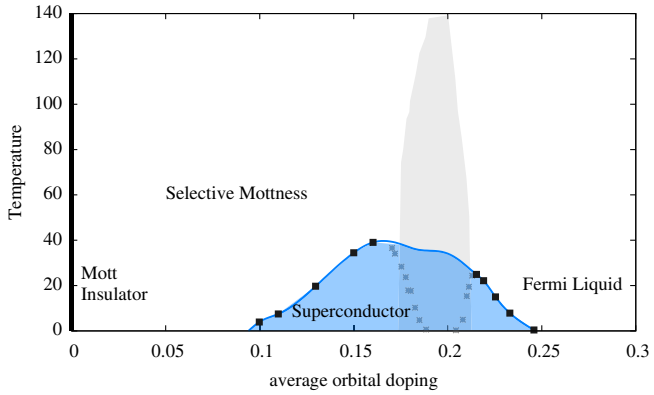

FIG. 3 (color online). Possible unified phase diagram for pnictides and cuprates. We plot here the experimental phase diagram for doped $BaFe_2As_2$ (from [45]) as a function of the average orbital doping. In the hypothesis that the magnetically ordered and orthorhombically distorted phase (light gray area) is accidentally favored by the total commensurate filling $n = 6$ around the stoichiometric compound thus suppressing the superconductivity of the tetragonal phase, we artificially eliminate it and complete the superconducting dome (blue area). We then see that this dome is centered around 20% doping (per orbital) away from the half-filled Mott insulator (here at $n = 5$), as in cuprates. In between, we find a strongly correlated Mott selective (and bad metallic [34]) phase, while at higher orbital dopings (corresponding, respectively, to the electron doped region in pnictides and the overdoped region in cuprates), we recover a moderately correlated Fermi liquid.

The authors acknowledge discussions with M. Aichhorn, R. Arita, E. Bascones, A. Georges, M. Imada, J. Mravlje, A. Millis, and E.Winograd. L. d. M. is funded by CNRS

and Agence Nationale de la Recherche under Program No. ANR-09-RPDOC-019-01. M. C. and G. G. are financed by ERC/FP7 through the Starting Independent Research Grant SUPERBAD (Grant No. 240524). Calculations have been performed at CINECA (HPC Project No. lsB06 SUPMOT).

Note added.—Recently, a careful investigation of the coherence scales in KFe_2As_2 revealed heavy-fermionic behavior[46], as predicted in our Letter.

[1] Y. Kamihara, T. Watanabe, M. Hirano, and H. Hosono, J. Am. Chem. Soc. **130**, 3296 (2008).
[2] I. I. Mazin, Nature (London) **464**, 183 (2010).
[3] D. C. Johnston, Adv. Phys. **59**, 803 (2010).
[4] W. L. Yang *et al.*, Phys. Rev. B **80**, 014508 (2009).
[5] I. I. Mazin, D. J. Singh, M. D. Johannes, and M. H. Du, Phys. Rev. Lett. **101**, 057003 (2008).
[6] Q. Si and E. Abrahams, Phys. Rev. Lett. **101**, 076401 (2008).
[7] K. Haule and G. Kotliar, New J. Phys. **11**, 025021 (2009).
[8] L. de' Medici, J. Mravlje, and A. Georges, Phys. Rev. Lett. **107**, 256401 (2011).
[9] M. D. Johannes and I. I. Mazin, Phys. Rev. B **79**, 220510 (2009).
[10] F. Hardy, P. Burger, T. Wolf, R. A. Fisher, P. Schweiss, P. Adelmann, R. Heid, R. Fromknecht, R. Eder, D. Ernst, H. v. Löhneysen, and C. Meingast, Europhys. Lett. **91**, 47008 (2010).
[11] P. Popovich, A. V. Boris, O. V. Dolgov, A. A. Golubov, D. L. Sun, C. T. Lin, R. K. Kremer, and B. Keimer, Phys. Rev. Lett. **105**, 027003 (2010).
[12] A. K. Pramanik, M. Abdel-Hafiez, S. Aswartham, A. U. B. Wolter, S. Wurmehl, V. Kataev, and B. Büchner, Phys. Rev. B **84**, 064525 (2011).
[13] G. Mu, H. Luo, Z. Wang, L. Shan, C. Ren, and H.-H. Wen, Phys. Rev. B **79**, 174501 (2009).
[14] J. S. Kim, E. G. Kim, G. R. Stewart, X. H. Chen, and X. F. Wang, Phys. Rev. B **83**, 172502 (2011).
[15] M. Abdel-Hafiez, S. Aswartham, S. Wurmehl, V. Grinenko, C. Hess, S.-L. Drechsler, S. Johnston, A. U. B. Wolter, B. Büchner, H. Rosner, and L. Boeri, Phys. Rev. B **85**, 134533 (2012).
[16] L. Degiorgi, New J. Phys. **13**, 023011 (2011).
[17] G. Li, W. Z. Hu, J. Dong, Z. Li, P. Zheng, G. F. Chen, J. L. Luo, and N. L. Wang, Phys. Rev. Lett. **101**, 107004 (2008).
[18] J. Yang, D. Hüvonen, U. Nagel, T. Rõ om, N. Ni, P. C. Canfield, S. L. Bud'ko, J. P. Carbotte, and T. Timusk, Phys. Rev. Lett. **102**, 187003 (2009).
[19] N. L. Wang, W. Z. Hu, Z. G. Chen, R. H. Yuan, G. Li, G. F. Chen, and T. Xiang, J. Phys. Condens. Matter **24**, 294202 (2012).
[20] V. Brouet, M. Fuglsang Jensen, A. Nicolaou, A. Taleb-Ibrahimi, P. Le Fevre, F. Bertran, A. Forget, and D. Colson, arXiv:1105.5604.
[21] M. Yi, D. H. Lu, J. G. Analytis, J.-H. Chu, S.-K. Mo, R.-H. He, R. G. Moore, X. J. Zhou, G. F. Chen, J. L. Luo, N. L. Wang, Z. Hussain, D. J. Singh, I. R. Fisher, and Z.-X. Shen, Phys. Rev. B **80**, 024515 (2009).
[22] H. Ding, K. Nakayama, P. Richard, S. Souma, T. Sato, T. Takahashi, M. Neupane, Y.-M. Xu, Z.-H. Pan, A. V. Fedorov, Z. Wang, X. Dai, Z. Fang, G. F. Chen, J. L. Luo, and N. L. Wang, J. Phys. Condens. Matter **23**, 135701 (2011).
[23] T. Yoshida, S. Ideta, I. Nishi, A. Fujimori, M. Yi, R. G. Moore, S. K. Mo, D.-H. Lu, Z.-X. Shen, Z. Hussain, K. Kihou, P. M. Shirage, H. Kito, C. H. Lee, A. Iyo, H. Eisaki, and H. Harima, arXiv:1205.6911.
[24] T. Terashima, M. Kimata, N. Kurita, H. Satsukawa, A. Harada, K. Hazama, M. Imai, A. Sato, K. Kihou, C.-H. Lee, H. Kito, H. Eisaki, A. Iyo, T. Saito, H. Fukazawa, Y. Kohori, H. Harima, and S. Uji, J. Phys. Soc. Jpn. **79**, 053702 (2010).
[25] L. de' Medici, S. R. Hassan, M. Capone, and X. Dai, Phys. Rev. Lett. **102**, 126401 (2009).
[26] L. de' Medici, S. Hassan, and M. Capone, J. Supercond. **22**, 535 (2009).
[27] S.-P. Kou, T. Li, and Z.-Y. Weng, Europhys. Lett. **88**, 17010 (2009).
[28] A. Hackl and M. Vojta, New J. Phys. **11**, 055064 (2009).
[29] W.-G. Yin, C.-C. Lee, and W. Ku, Phys. Rev. Lett. **105**, 107004 (2010).
[30] See Supplemental Material at http://link.aps.org/supplemental/10.1103/PhysRevLett.112.177001 for details of the experimental analysis, a survey of the theoretical framework and method used, and a complete discussion of the analysis of the DCA calculations of Ref. [32] in terms of the orbital decoupling mechanism.
[31] M. M. Qazilbash, J. J. Hamlin, R. E. Baumbach, L. Zhang, D. J. Singh, M. B. Maple, and D. N. Basov, Nat. Phys. **5**, 647 (2009).
[32] E. Gull, M. Ferrero, O. Parcollet, A. Georges, and A. J. Millis, Phys. Rev. B **82**, 155101 (2010).
[33] A. Georges, L. de' Medici, and J. Mravlje, Annu. Rev. Condens. Matter Phys. **4**, 137 (2013).
[34] H. Ishida and A. Liebsch, Phys. Rev. B **81**, 054513 (2010).
[35] R. Yu and Q. Si, Phys. Rev. B **86**, 085104 (2012).
[36] N. Lanatà, H. U. R. Strand, G. Giovannetti, B. Hellsing, L. de' Medici, and M. Capone, Phys. Rev. B **87**, 045122 (2013).
[37] Z. P. Yin, K. Haule, and G. Kotliar, Nat. Mater. **10**, 932 (2011).
[38] M. Aichhorn, L. Pourovskii, V. Vildosola, M. Ferrero, O. Parcollet, T. Miyake, A. Georges, and S. Biermann, Phys. Rev. B **80**, 085101 (2009).
[39] A. Liebsch and H. Ishida, Phys. Rev. B **82**, 155106 (2010).
[40] P. Werner, M. Casula, T. Miyake, F. Aryasetiawan, A. J. Millis, and S. Biermann, Nat. Phys. **8**, 331 (2012).
[41] P. Werner, E. Gull, M. Troyer, and A. J. Millis, Phys. Rev. Lett. **101**, 166405 (2008).
[42] L. de' Medici, Phys. Rev. B **83**, 205112 (2011).
[43] H. Ikeda, R. Arita, and J. Kuneš, Phys. Rev. B **82**, 024508 (2010).
[44] T. Misawa, K. Nakamura, and M. Imada, Phys. Rev. Lett. **108**, 177007 (2012).
[45] S. Avci, O. Chmaissem, D. Y. Chung, S. Rosenkranz, E. A. Goremychkin, J. P. Castellan, I. S. Todorov, J. A. Schlueter, H. Claus, A. Daoud-Aladine, D. D. Khalyavin, M. G. Kanatzidis, and R. Osborn, Phys. Rev. B **85**, 184507 (2012).
[46] F. Hardy, A. E. Boehmer, D. Aoki, P. Burger, T. Wolf, P. Schweiss, R. Heid, P. Adelmann, Y. X. Yao, G. Kotliar, J. Schmalian, and C. Meingast, Phys. Rev. Lett. **111**, 027002 (2013).